

THE ROLE OF GRID CELL SIZE, FLOW ROUTING ALGORITHM AND SPATIAL VARIABILITY OF SOIL DEPTH ON SHALLOW LANDSLIDE PREDICTION

T. UCHIDA^(*), K. TAMUR^(*) & K. AKIYAMA^(*)

^(*)Public Works Research Institute, Ibaraki, Japan

ABSTRACT

To assess the spatial pattern of landslide susceptibility, we linked a simple hydrological model and an infinite slope stability model to predict the spatial pattern of critical steady-state rainfall required to cause slope instability. We studied a headwater in the Aratani River basin, western Japan. To clarify soil depth spatial patterns, we measured soil depth on the hillslope by using knocking pole tests. We compared two widely used procedures for determining local slope angle and upslope contributing area: a single-flow-direction procedure and an algorithm based on proportioning flow into two downslope pixels. Further, we examined the role of the analysis grid cell size on the precision of landslide prediction. We showed that by choosing an optimal grid cell size and using an optimal procedure for calculation of the upslope contributing area and by performing a detailed field survey to determine soil depth, the precision of landslide susceptibility assessment could be remarkably improved

KEY WORDS: *shallow landslide, soil depth, physically based model, grid cell size, procedure for calculation of topographic indices*

INTRODUCTION

Shallow landslides are one of the key processes that cause debris flows. Therefore, predicting where landslides are likely to occur is key to preventing debris flow disasters. Since the pioneering work of

Okimura, several physically based models predicting shallow landslide susceptibility have been developed, and such models are potentially a powerful way to evaluate the spatial pattern of shallow landslide susceptibility (e.g., OKIMURA *et alii*, 1985; HIRAMATSU *et alii*, 1990; MONTGOMERY & DIETRICH, 1994; WU & SIDLE, 1995; PACK *et alii*, 1998; KOSUGI *et alii*, 2002; ROSSO *et alii*, 2006; TAROLLI & TARBOTON, 2006; TALEBI *et alii*, 2007).

These models were developed from models of slope stability and subsurface water flow. One of the simplest approaches combines an infinite slope stability analysis with a steady-state shallow subsurface flow model (e.g., OKIMURA *et alii*, 1985; MONTGOMERY & DIETRICH, 1994; PACK *et alii*, 1998). Recently, more complex processes of shallow landslide occurrence have been incorporated into physically based models predicting the spatial patterns of shallow landslide susceptibility (e.g., HIRAMATSU *et alii*, 1990; WU & SIDLE, 1995; ROSSO *et alii*, 2006; TALEBI *et alii*, 2007). For example, WU & SIDLE (1995) and ROSSO *et alii* (2006) incorporated temporal change of lateral subsurface flow into their models, and HIRAMATSU *et alii* (1990) and KOSUGI *et alii* (2002) considered the effects of water flow and storage in vadose zones, thus improving the precision of landslide susceptibility prediction by the models.

Although complex processes can be described by numerical simulations, such models require that the spatial patterns of many parameters be specified.

However, detailed below-ground information about the values of such parameters as bedrock topography, soil depth, soil mechanical parameters, and soil hydraulic parameters, have generally been lacking. So, it can be thought that even though the complex numerical simulation models, most of processes can not fully described, since the parameters controls these processes cannot be measured. WHILE, OKIMURA *et alii* (1985) and MONTGOMERY & DIETRICH (1994) indicated that the simple model combines an infinite slope stability analysis with a steady-state shallow subsurface flow was used as a reasonable approximation of a shallow landslide occurrence.

In most simulations for predicting landslide locations, many parameter values have been determined by back-calculations or by calibration against past observed events, which often were represented by mean values of a limited number of observed data. For example, although soil depth exerts a first-order control on shallow landslide potential on steep hillslopes (e.g., DIETRICH *et alii*, 1995; IDA, 1999), landslide prediction studies have often interpolated soil depth from a limited number of field measurements (e.g., HIRAMATSU *et alii*, 1990; MONTGOMERY & DIETRICH, 1994; WU & SIDLE, 1995; TAROLLI & TARBOTON, 2006). Further, recent hillslope hydrology studies have shown that on steep, wet, soil-mantled hillslopes, the bedrock surface and not the ground surface topography may be the most important surface controlling the routing of mobile water laterally downslope (e.g., FREER *et alii*, 2002). Moreover, it is likely that the landslide slip surface is also strongly controlled by bedrock surface topography. Most landslide prediction studies have used a ground surface digital elevation model (DEM) to calculate values of parameters used as topographic indexes, such as local slope angle and upslope contributing area, because information about the bedrock surface topography is often lacking.

Moreover, the method and grid cell size used for calculation of topographic index values can be expected to affect the precision of shallow landslide assessment. TAROLLI & TARBOTON (2006) have recently demonstrated the effect of grid cell size on the precision of shallow landslide assessment and the optimal grid cell size in Miozza catchment in north-eastern Italy was 10 m. In addition, researchers have proposed a variety of procedures as optimal for calculation of upslope contributing area by hydrological models (e.g., TARBOTON,

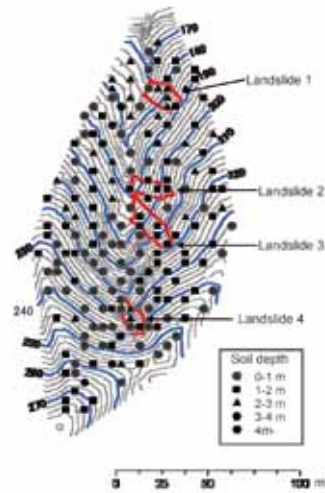


Fig. 1 - Topography and soil depth of the Aratani hillslope study site

1997). However, most of these previous studies did not examine in detail the optimal grid cell size or upslope contributing area calculation to use for assessing landslide susceptibility.

We propose three hypotheses, i.e., that the precision of shallow landslide susceptibility assessment by a physically based model could be improved by (1) choosing the optimal grid cell size; (2) using the optimal method for calculating topographic index parameter values; and (3) inputting more detailed information about (a) soil depth and (b) bedrock surface topography. Here, we examine these hypotheses by comparing model results obtained by using grid cell sizes from 5 to 25 m and between two different methods for calculating topographic indexes, and by conducting a detailed field survey to obtain data on soil depth and bedrock surface topography and then comparing results obtained by using bedrock surface topography with those obtained by using ground surface topography.

STUDY SITE

We conducted a detailed field investigation of a hillslope site in the upper Aratani River basin in the western Hiroshima Mountains, western Japan (Fig. 1). The region is humid and temperate: the mean annual precipitation in this region is around 1700 mm, and the mean temperature is around 15 °C. The site is deeply incised and dominated by hillslopes, with no riparian area. Slope angles range from 20 to 45°, and

slope lengths from 30 to 100 m. The area is underlain by Hiroshima Granite, and the soils are sandy. The site is covered by secondary forest, predominately *Pinus densiflora*. Specific weights of saturated (17.9 kN/m³) and unsaturated (15.1 kN/m³) soil and the soil friction angle (36.1°) of the Aratani hillslope were previously measured in the laboratory in five undisturbed 100 cm³ field cores (UCHIDA *et alii*, 2009).

On 29 June 1999, more than 7000 shallow landslides occurred in the western Hiroshima Mountains, and these landslides triggered many debris flows. Four of these shallow landslides occurred in the study area. The landslide scars range from 9 to 15 m in width. The total rainfall amount and maximum rainfall intensity of the triggering event were 417 mm and 63 mm/h, respectively, measured at Uokiri dam (1.4 km north of Aratani).

Hydrometric observations of groundwater level, soil pore water pressure, soil water content, and stream flow rate have been conducted on the hillslope since 2003 (UCHIDA *et alii*, 2009). These hydrometric observations showed that except for the driest period, the surface water flow can be observed at the lower end of the catchment. Stream water was sensitive to rainfall intensities during storm runoff. Groundwater level and soil pore water pressure measurements showed that within most of the hillslope area, the soil-bedrock interface was not commonly saturated between events. Several monitored large storms produced saturation at the soil-bedrock interface and the soil pore pressures were sensitive to the rainfall intensity.

METHOD

THEORY

We calculated the critical steady-state rainfall required to cause shallow landsliding following the methods of OKIMURA *et alii* (1985) and MONTGOMERY & DIETRICH (1994). An infinite planar slope can be used as a good approximation of a hillslope when the soil depth is small with respect to the length of the slope, as in the case of our hillslope (e.g., OKIMURA *et alii*, 1985; MONTGOMERY & DIETRICH, 1994; WU & SIDLE, 1995; ROSSO *et alii*, 2006). Thus, if saturated depth is less than soil depth, an infinite slope stability analysis can be used to compute the factor of safety (FS) as follows:

$$FS = \frac{c + (\gamma_w \cos^2 I - h_s \gamma_w \cos^2 I) \tan \phi}{\gamma_w \cos I \cdot \sin I} \quad (1)$$

where c is effective cohesion, ϕ is the friction angle of the soil mantle, I is the angle of the bedrock surface, γ and γ_w are the specific weights of soil mantle and water, respectively, and h and h_s are the soil and saturated water depths, respectively. We assumed that γ can be described by the equation

$$\gamma = \frac{\gamma_s h_s + (h - h_s) \gamma_t}{h} \quad (2)$$

where γ_s and γ_t are the specific weights of saturated and unsaturated soil, respectively.

According to Darcy's law, the saturated water depth, h_s , at a given steady-state rainfall intensity, r , can be described as

$$h_s = \frac{rA}{K_s \sin I \cos I} \quad (3)$$

where A is the contributing area of the unit contour length, and K_s is the saturated hydraulic conductivity of the soil mantle. Therefore, if $h \leq h_s$, then the critical steady-state rainfall required to cause shallow landsliding, r_c , can be determined with equations 1 through 3 by setting $FS = 1$, as follows:

$$r_c = \frac{K_s \tan I \cos I \{c - \gamma_t h \cos I (\sin I - \cos I \tan \phi)\}}{A \{ \gamma_w \cos I \tan \phi + (\gamma_s - \gamma_t) (\sin I - \cos I \tan \phi) \}} \quad (4)$$

FIELD MEASUREMENTS

We measured the surface topography using LiDAR (light detection and ranging) data and developed a 1-m DEM. We also mapped the edges of the shallow landslides that occurred in June 1999 during a field survey (Fig. 1). Soil depth on the Aratani hillslope was measured with a cone penetrometer (knocking pole test) with a cone diameter of 25 mm, a weight of 5 kg, and a fall distance of 50 cm. N_d represents the number of blows required for 10 cm of penetration. Knocking pole tests were conducted at intervals of 10–15 m in 2005. In all, we conducted the tests at 181 points, 16 of which were on the shallow landslide scars (Fig. 1).

The knocking pole test results on the shallow landslide scars where weathered bedrock was exposed showed that the N_d value of weathered bedrock was around 20, indicating that a layer with an N_d of less than 20 can potentially fail, causing a shallow landslide. Therefore, in this study we assumed that N_d values greater than 20 indicated bedrock and we defined the depth of the layer with $N_d < 20$ as the soil depth.

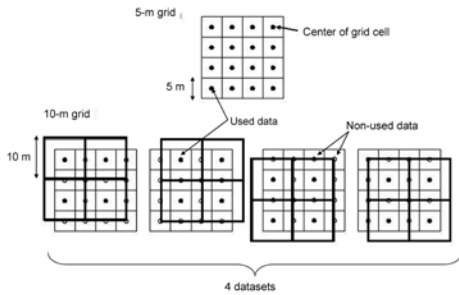


Fig. 2 - Schematic illustration of grid cell creation. Circle represents center of grid which has elevation data. Black and white circles in the lower panel represent used and non-used data, respectively. Bold and solid lines in the lower panel represent created 10-m grid and original 5-m grid, respectively

ANDERSON *et alii* (1997) and UCHIDA *et alii* (2003) defined bedrock as a layer that cannot be penetrated with a hand auger. The depth of the layer with $N_d < 20$ was almost the same as the depth of the layer that could be penetrated with a hand auger, so our definition is consistent with that of ANDERSON *et alii* (1997) and UCHIDA *et alii* (2003).

DATA PREPARATION

TOPOGRAPHY

Since we conducted our field survey after the shallow landslides had occurred, we interpolated the pre-landslide surface topography across the landslide scars on the 1-m DEM. In addition, we made the 5-m DEM of the ground surface from the 1-m DEM made using the LiDAR data. Then, we used a Kriging interpolation scheme to make a 5-m DEM of the bedrock surface from a 5-m ground surface DEM and the soil depth data. Thus, we calculated slope angle and upslope drainage area data sets for both the ground surface topography and the bedrock surface topography. Also, we compiled a 5-m-grid soil depth data set by subtracting the bedrock surface elevation from the ground surface elevation at each grid point.

To determine the most effective DEM resolution for assessing shallow landsliding susceptibility at this study site, we made DEMs of the bedrock surface topography at three additional grid cell sizes (10, 15, and 25 m) using a Kriging interpolation scheme. We made 4, 9, and 25 datasets for the 10-, 15-, and 25-m DEMs, respectively (see an example of 10-m DEM in Fig. 2) so that the same number of elevation data was used to

	Grid size	Soil depth	Procedure*	DEM*
Case 1	5 m	Observed	D-infinity	Bedrock surface
Case 2	10 m	Observed	D-infinity	Bedrock surface
Case 3	15 m	Observed	D-infinity	Bedrock surface
Case 4	25 m	Observed	D-infinity	Bedrock surface
Case 5	5 m	Observed	D8	Bedrock surface
Case 6	5 m	Observed	D-infinity	Ground surface
Case 7	5 m	Averaged	D-infinity	Bedrock surface
Case 8	5 m	Averaged	D-infinity	Ground surface

*Method used to calculate slope angle and upslope contributing

Tab 1 - Simulated case

calculate rc in each case.

Various procedures are available for calculating topographic indexes. Here, we compared two widely used procedures for determining local slope angle and upslope contributing area, a single-flow-direction procedure (hereafter referred to as D8; O'CALLAGHAN & MARK, 1984) and an algorithm based on proportioning flow between two downslope pixels (hereafter referred to as D-infinity; TARBOTON, 1997). In D8, the flow direction is computed by assigning flow from each pixel to one of its eight neighbours, either adjacent or diagonal, in the direction with steepest downward slope. While, D-infinity is based on representing flow direction as a single angle taken as the steepest downward slope on the eight triangular facets centred at each grid point. Upslope area is then calculated by proportioning flow between two downslope pixels according to how close this flow direction is to the direct angle to the downslope pixel (TARBOTON, 1997).

SOIL MANTLE PARAMETERS

The friction angle and the specific weights of saturated and unsaturated soil were measured in undisturbed soil samples. Soil cohesion was estimated by using data on both soil depth and topography. We assumed that if the soil mantle was unsaturated ($h_s = 0$), the factor of safety of most grid cells would be larger than 1.0. Therefore, we used equations 1 and 2 to calculate the minimum cohesion, including root strength, required for all grid cells to remain stable, excepting one grid cell where the soil was very deep and the local slope was very steep. We also back-calculated cohesion for each of our test cases (Tab. 1, see below) as the minimum cohesion required for all grid cells to remain stable. The calculated cohesion data are shown in Table 2.

Effective hillslope saturated conductivity (transmissivity) is often different from soil saturated con-

Saturated hydraulic conductivity [m/s]	0.0005
Cohesion [kN/m ²]	
Case 1	7.7
Case 2	5
Case 3	4.8
Case 4	3.6
Case 5	7.3
Case 6	9
Case 7	5.7
Case 8	5.7
Friction angle [°]	36.1
Specific weights of saturated soil [kN/m ³]	17.9
Specific weights of unsaturated soil [kN/m ³]	15.2
Specific weights of water [kN/m ³]	9.8

Tab 2 - Parameter values

ductivity measured in a small undisturbed soil sample (e.g., BAZEMORE *et alii*, 1994; UCHIDA *et alii*, 2003). Therefore, using the method of BAZEMORE *et alii* (1994) and UCHIDA *et alii* (2003), we estimated the saturated conductivity of the soil (K_s) as the effective hillslope saturated conductivity by using the observed total amount of subsurface flow discharge and the mean soil pore pressure in the lower part of the hillslope. Such an estimate can be made assuming the applicability of Darcy's law

$$K_s = Q_s A \frac{dh}{dl} \quad (5)$$

where Q_s is total amount of subsurface flow discharge, A is the flux area, and dh/dl is the hydraulic gradient. We assumed that the Q_s is equal to the total runoff from the study site which measured at the lower end of the site. The hydraulic gradient (dh/dl) of 0.72 was assumed to be equal to the mean surface gradient in the hillslope. The width and the depth of the flux area were assumed to be equal to the twice of ephemeral stream length and the observed soil pore water pressure head at the lower part of the hillslope, respectively. Using the hydrometric data of the heaviest rainfall during the observation period (total rainfall, 236 mm; maximum rainfall intensity, 53 mm/h), we calculated K_s of the Aratani hillslope to be 5.2×10^{-4} m/s, which is 17 times the averaged soil saturated conductivity measured in the undisturbed 100 cm³ soil samples of UCHIDA *et alii* (2009)

SIMULATED CASES AND DATA ANALYSIS

We summarize the simulated cases in Table 1, and the values of the parameters used for the calculations in Table 2. Briefly, we compared the effects of grid cell size in Cases 1–4 and the effect of the calculation

procedure for topographic indexes in Cases 1 and 5. We compared differences between detailed and less detailed soil data and between use of the ground surface instead of the bedrock surface in Cases 1 and 6–8. We used r_c , the critical steady-state rainfall amount, as an index for assessing shallow landslide susceptibility. We interpreted grid cells with lower r_c values to be more susceptible to shallow landsliding, and those with higher r_c to be more stable, because the higher the r_c value was, the less frequent would be the occurrence of a rainfall event sufficient to cause shallow landsliding.

To test model performance, we compared simulated r_c values in observed landslide areas by calculating the “landslide ratio,” as follow. If the centre of a given grid cell was inside an observed landslide polygon, we defined the grid cell as a landslide cell. We defined the ratio of landslide grid cells to all grid cells as landslide ratio.

By setting $h_s = h$ in equation 3 and rearranging, the fully saturated condition can be described as follows:

$$r = \frac{hK_s \sin I \cos I}{A} \quad (6)$$

Thus, if a grid cell satisfies the equation

$$\frac{c}{\gamma_w \cos^2 I \tan \phi + \gamma_s \cos I (\sin I - \cos I \tan \phi)} > h \quad (7)$$

even if the soil mantle is fully saturated, FS is larger than 1.0. Therefore, we interpreted such grid cells as “unconditionally stable” with regard to shallow landsliding, and other grid cells as “potentially unstable.” Then, we calculated landslide ratio for grid cells which grouped into “unconditionally stable” and “potentially unstable”, respectively.

Also, we examine the effectiveness of r_c on predictions of the landslide susceptibility of potentially unstable cells. We calculated the landslide ratio and mean r_c for a 20-value moving window of grid cells sorted by r_c as follow. According to equation 4 the absolute value of r_c is strongly controlled by K_s . Thus, first, we sorted potentially unstable cell according to the simulated r_c . Then, we picked up 20-grid cells from the first grid cell which has the smallest r_c to the 20th grid cell and calculated the landslide ratio and mean r_c for these 20-grid cells. Next, we calculated

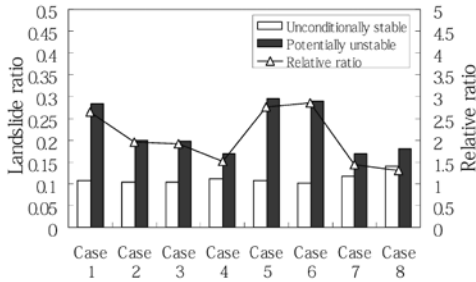


Fig. 3 - Landslide ratios and relative ratio (the ratio of potentially unstable landslide ratio to the unconditionally stable landslide ratio)

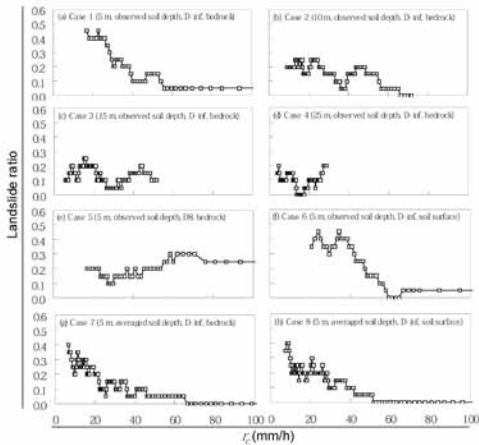


Fig. 4 - Relationship between r_c and landslide ratio

the landslide ratio and mean r_c for the next 20-grid cells which means grid cells from 2nd to 21st grids according to the order of simulated r_c . We conducted this calculation continuously. We interpreted a clear inverse relationship between r_c and the landslide ratio and a large difference in the landslide ratio between potentially unstable cells and unconditionally stable cells to demonstrate better model performance.

RESULTS

In the Case 1 the landslide ratio of unconditionally stable cells was 0.11, whereas that of potentially unstable cells was 0.28 (Fig. 3). We observed a clear inverse relationship between r_c and the landslide ratio (Fig. 4a). These results indicate that the predicted r_c of Case 1 well described landslide locations and the rainfall amount required to cause shallow landslide. In the Case 1 simulation result, in at least one mesh in each landslide scar, r_c was smaller than the observed maximum 1-hour rainfall (63 mm/h) (Fig.

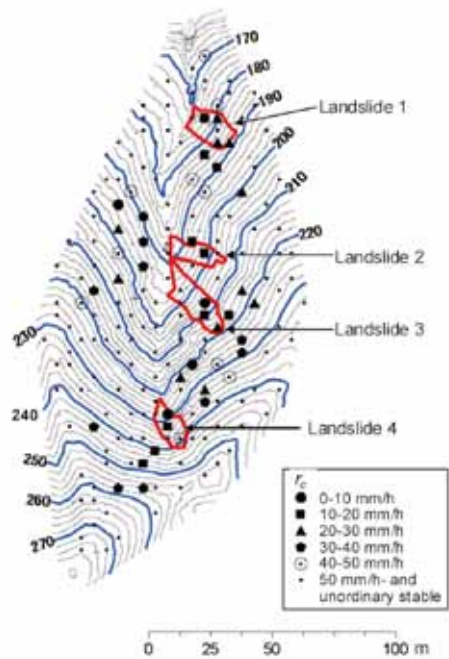


Fig. 5 - Spatial pattern of simulated r_c in Case 1

5). Predicted r_c values were generally large outside the landslide area.

When the grid cell size was set to 10 m (Case 2), the landslide ratio of unconditionally stable cells remained around 0.11, whereas that of potentially unstable cells was 0.20 (Fig. 3). There was a weak inverse relationship between r_c and the landslide ratio, but the apparent slope of the relationship was smaller than it was in Case 1 (Fig. 4b). Further, in Cases 3 (15-m grid cell) and 4 (25-m grid cell), the landslide ratio differed between unconditionally stable grid cells (0.10 and 0.11 in Cases 3 and 4, respectively) and potentially unstable grid cells (0.20 and 0.17, respectively) (Fig. 3). However, r_c and the landslide ratio did not show a clear inverse relationship (Figs. 4c and 4d).

When we used D8 to determine the landslide ratios of unconditionally stable and potentially unstable grid cells were 0.11 and 0.30, respectively (Fig. 3), almost the same as those of Case 1. However, there was no clear inverse relationship between r_c and the landslide ratio (Fig. 4e).

When we used a ground surface DEM (Case 6), instead of a bedrock surface DEM, the predicted r_c was similar to that of Case 1, so there was a large difference in the landslide ratio between unconditionally

stable (0.10) and potentially unstable (0.29) grid cells (Fig. 3). Further, there was a clear inverse relationship between r_c and the landslide ratio, also similar to Case 1 (Fig. 4f).

When we used averaged soil depth (Cases 7 and 8), instead of the observed soil depth at each measurement point, the differences in the landslide ratio between unconditionally stable (0.12 and 0.14 in Cases 7 and 8, respectively) and potentially unstable (0.17 and 0.18) grid cells were small (Fig. 3). Although the landslide ratio clearly decreased as the predicted r_c increased (Figs. 4g and 4h), the landslide ratios of grid cells with $r_c = 20\text{--}30$ mm/h were similar to those of unconditionally stable grid cells; thus, the landslide ratios of grid cells with $r_c = 30\text{--}100$ mm/h were smaller than those of unconditionally stable grid cells.

DISCUSSION

ROLE OF GRID CELL SIZE

The relative landslide ratio of potentially unstable to unconditionally stable grid cells decreased as grid cell size increased (Fig. 3, Cases 1–4). We observed an inverse relationship between predicted r_c and the landslide ratio, however, only in Cases 1 (5-m grid) and 2 (10-m grid), indicating that when a grid cell size of 15 m or greater is used, the predicted r_c is useful only for determining whether a grid cell is unconditionally stable. These results suggest that the most effective grid cell size at this study site is around 5 m.

TAROLLI & TARBOTON (2006), who also examined the optimal grid cell size for assessing shallow landslide susceptibility using a physically based model, reported that the optimal grid cell size at their site was 10 m. IWAHASHI *et alii* (2009) investigated the optimal grid cell size for assessing shallow landslide susceptibility by discriminant analysis and reported that it was strongly controlled by landslide size. Our result is consistent with these findings, because both the optimal grid cell size and the landslide size on our hillslope are smaller than those reported by TAROLLI & TARBOTON (2006).

CALCULATION PROCEDURE FOR FLOW ROUTING

TARBOTON (1997) and BORGA *et alii* (2004) reported that D-infinity performed better than D8 in calculating the upslope contributing area. Here we showed that even when the input data, including the

DEM, were the same, an inverse relationship between predicted r_c and the landslide ratio was not obtained when D8 was used, whereas when D-infinity was used, a clear inverse relationship resulted. Both calculation procedures, however, resulted in a large difference in the landslide ratio between unconditionally stable and potentially unstable grid cells.

The equation 6 indicates that the conditions of unconditionally stable and potentially unstable grid cells are not affected by the upslope contributing area, which is determined by the local slope angle, soil depth, and soil properties, whereas equation 4 shows that the upslope contributing area does affect the predicted r_c . These results indicate that the effectiveness of D-infinity in calculating the upslope contributing area, as reported by TARBOTON (1997) and BORGA *et alii* (2004), improves the precision with which shallow landslide susceptibility can be determined. D8, in contrast, can reasonably distinguish between unconditionally stable and potentially unstable grid cells because the upslope contributing area does not affect this determination.

BEDROCK SURFACE VERSUS GROUND SURFACE TOPOGRAPHY

Because the bedrock surface topography controls the routing of subsurface flow (e.g., FREER *et alii*, 2002), we expected the precision of landslide prediction to be improved by using the bedrock topography instead of the ground surface topography. However, predicted r_c calculated using the ground surface DEM (Case 6) was almost the same as that calculated using the bedrock surface DEM (Case 1). Thus, the difference between the ground surface and bedrock surface DEMs had little effect on the precision of landslide susceptibility prediction. We think it likely therefore that the difference between these two DEMs is small on the Aratani hillslope.

SPATIAL VARIABILITY OF SOIL DEPTH

Observed soil depth varied greatly spatially (Fig. 1). When we ignored the spatial variability of soil depth by using averaged depths, grid cells with lower r_c (<20 mm/h) had higher landslide ratios than grid cells with higher r_c or unconditionally stable grid cells. However, the landslide ratio did not differ between grid cells with higher r_c (>20 mm/h) and unconditionally stable grid cells. We showed the relationship between

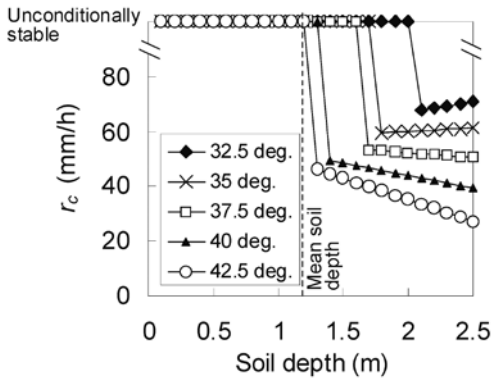


Fig. 6 - Relationship between soil depth and r_c calculated using parameters for Case 1 and $25 \text{ m}^2/\text{m}$ of upslope contributing area

tween soil depth and r_c calculated using parameters for Case 1 and $25 \text{ m}^2/\text{m}$ of upslope contributing area (Fig. 6). This figure showed that effects of soil depth on r_c were not so large, if the grid cell categorized as potentially unstable. While, the conditions of unconditionally stable and potentially unstable grid cells are strongly affected by the soil depth. That is, if the averaged soil depth was used instead of observed soil depth, several potentially unstable grid cells predicted by using observed soil depth were assessed as unconditionally stable. These results indicate that if we ignore the spatial variability of soil depth, the precision of distinguishing between unconditionally stable and potentially unstable grid cells becomes worse.

Many previous studies have shown large spatial variability in soil depth on individual hillslopes or

mountains (e.g., OKIMURA, 1989; IIDA & TANAKA, 1997; HEIMSATH *et alii*, 1997; FREER *et alii*, 2002; TESFA *et alii*, 2009). Therefore, spatial variability in soil depth is likely to be important in determining shallow landslide susceptibility on other steep landscapes.

CONCLUSIONS

We examined the hypothesis that a detailed field survey of soil depth distribution and bedrock surface topography, and the choice of an optimal grid cell size and topographic index calculation procedure, can improve the precision of shallow landslide susceptibility assessment. We showed that the choice of an optimal grid cell size and an optimal procedure for calculating the upslope contributing area, and a detailed field survey of soil depth remarkably improves the precision of landslide susceptibility assessment. Use of a ground surface DEM instead of a bedrock surface DEM, however, had little effect on the precision of landslide susceptibility prediction. These findings indicate that the existing simple models, if an optimal grid cell size and procedure for topographic index calculation are chosen and a detailed field survey is conducted, can yield results useful for landslide susceptibility assessment. We consider, of course, that improvement of numerical simulation models is important, but this study shows that detailed field surveys to clarify the spatial variability of soil depth and fine-resolution topographic measurements and hydrometric observations are also very important to improve the precision of landslide susceptibility assessment.

REFERENCES

- ANDERSON S.P., DIETRICH W.E., MONTGOMERY D.R., TORRES R., CONRAD M.E. & LOAGUE K. (1997) - *Subsurface flow paths in a steep unchanneled catchment*. Water Resour. Res.: **33**: 2637–2653.
- BAZEMORE D.E., ESHLEMAN K.N. & HOLLENBECK L.J. (1994) - *The role of soil water in stormflow generation In a forested head-water catchment: synthesis of natural tracer and hydrometric evidence*. J. Hydrol.: **162**: 47–75.
- BORGA M., TONELLI F. & SELLERONI J. (2004) - *A physically based model of the effects of forest roads on slope stability*. Water Resour. Res.: **40**, doi:10.1029/2004WR003238.
- DIETRICH W.E., REISS R., HSU M.-L. & MONTGOMERY D.R. (1995) - *A process-based model for colluvial soil depth and shallow landsliding using digital elevation data*. Hydrol. Processes: **9**: 383–400.
- FREER J., McDONNELL J.J., BEVEN K.J., PETERS N.E., BURNS D.A., HOOPER R.P., AULENBACH B. & KENDALL C. (2002) - *The role of bedrock topography on subsurface storm flow*. Water Resour. Res.: **38**, doi: 10.1029/2001WR000872.
- HEIMSATH A.M., DIETRICH W.E., NISHIZUMI K. & FINKEL R.C. (1997) - *The soil production function and landscape equilibrium*. Nature: **388**: 358–361.
- HIRAMATSU S., MIZUYAMA T. & ISHIKAWA, Y. (1990) - *Study of a method for predicting hillside landslides by analysis of transient flow of water in saturated and unsaturated soils*. J. Japan Soc. Erosion Control Eng.: **43**(1): 5–15.
- IIDA T. (1999) - *A stochastic hydro-geomorphological model for shallow landsliding due to rainstorm*. CATENA: **34**: 293–313.

- IIDA T. & TANAKA K. (1997) - *The relationship between topography and soil depth measured with the portable penetration test apparatus*. Trans. Jpn Geomorph. Un.: **18**: 61-78.
- IWAHASHI J., KAMIYA I. & YAMAGISHI H. (2009) - *Estimation of the Most Suitable Window Size of the Slope Gradient and Convexo-Concave Index for the Assessment of Shallow Landslides Using High-Resolution LiDAR DEM*. Trans. Jpn Geomorph. Un.: **30**: 15-27.
- KOSUGI K., MIZUYAMA, T. & FUJITA, M. (2002) - *Accuracy of a shallow landslide prediction model to estimate groundwater table*. J. Japan Soc. Erosion Control Eng.: **55**(3), 21-32
- MONTGOMERY D.R. & DIETRICH W.E. (1994) - *A physically based model for the topographic control on shallow landsliding*. Water Resour. Res.; **30**: 1153–1171.
- O'CALLAGHAN J.F. & MARK D.M. (1984) - *The extraction of drainage networks from digital elevation data*. Comput. Vision Graphics Image Process.: **28**: 328–344.
- OKIMURA T. (1989) - *A method for estimating potential failure depth used for a probable failure predicting model*. J. Japan Soc. Erosion Control Eng.: **42**(1): 14-21.
- OKIMURA T., ICHIKAWA R. & FUJII, I. (1985) - *Methods to Predict Failures on Granite Mountain Slopes by a Infiltrated Water Movement Model in a Surface Layer*. J. Japan Soc. Erosion Control Eng. **37**(5): 44–49
- PACK R.T., TARBOTON D.G. & GOODWIN C.N. (1998) - *The SINMAP Approach to Terrain Stability Mapping*. 8th Congress of the International Association of Engineering Geology, Vancouver, British Columbia, Canada.
- ROSSO R., RULLI M.C. & VANNUCCHI G. (2006) - *A physically based model for the hydrologic control on shallow landsliding*. Water Resour. Res.: **42**, doi:10.1029/2005WR004369.
- TALEBI A., UIJLENHOET R. & TROCH P.A. (2007) - *Soil moisture storage and hillslope stability*. Nat. Hazards Earth Syst. Sci., **7**: 523–534.
- TARBOTON D.G. (1997) - *A new method for the determination of flow directions and upslope areas in grid digital elevation models*. Water Resour. Res.: **33**: 309-319.
- TAROLLI P. & TARBOTON D.G. (2006) - *A new method for determination of most likely landslide initiation points and the evaluation of digital terrain model scale in terrain stability mapping*. Hydrol. Earth Syst. Sci., **10**: 663-677.
- TESFA T.K., TARBOTON D.G., CHANDLER D.G. & McNAMARA J.P. (2009) - *Modeling soil depth from topographic and land cover attributes*. Water Resour. Res., **45**: doi: 10.1029/2008WR007474.
- UCHIDA T., ASANO Y., OHTE N. & MIZUYAMA T. (2003) - *Seepage area and rate of bedrock groundwater discharge at a granitic unchanneled hillslope*. Water Resour. Res., **39**: doi: 10.1029/2002 WR001298.
- UCHIDA T., MORI N., TAMURA K., TAKIGUCHI S. & KAMEE K. (2009) - *The role of data preparation on shallow landslide prediction*. J. Japan Soc. Erosion Control Eng.: **62** (1): 23-31.
- WU W. & SIDLE R.C. (1995) - *A distributed slope stability model for steep forested basins*. Water Resour. Res.: **31**: 2097-2110.